ELSEVIER

Available online at www.sciencedirect.com

SciVerse ScienceDirect

Ceramics International 38 (2012) 4819–4826

CERAMICS INTERNATIONAL

www.elsevier.com/locate/ceramint

Effect of preparation route on the properties of slip-casted Al_2O_3/YAG composites

F. Sommer [a,*], F. Kern [a], H.F. El-Maghraby [b], M. Abou El-Ezz [c], M. Awaad [b], R. Gadow [a], S.M. Naga [b]

[a] *Institut für Fertigungstechnologie Keramischer Bauteile, Universität Stuttgart, (Institute for Manufacturing Technologies of Ceramic Components and Composites, University of Stuttgart) Allmandring 7b, D-70569 Stuttgart, Germany*

[b] *Ceramics Department, National Research Centre (NRC), 12622 Dokki, Giza, Egypt*

[c] *Graduate School of excellence for advanced Manufacturing Engineering, Stuttgart University, Allmandring 7b, D-70569, Germany*

Received 13 December 2011; received in revised form 20 February 2012; accepted 23 February 2012

Available online 3 March 2012

Abstract

Alumina composites containing 5, 10 and 20 vol.% YAG were produced by a slip-casting process. Two different routes for adding the YAG phase were chosen. Either by mixing of alumina with previously produced YAG powder or by coating of an adequate amount of yttria to form YAG precipitates during the calcining step. The mechanical properties of the sintered samples were measured and compared. Independent from the preparation route Al_2O_3/10 vol.% YAG composites showed best mechanical properties. Significant differences in the densification behavior appeared between the two different manufacturing technologies. The presence of intermediately formed phases like YAM and YAP during the powder preparation step of coated composites is probably the reason why mixed composites showed higher mechanical properties than coated composites.

Keywords: A. Slip casting; B. Microstructure-final; B. Nanocomposites; C. Mechanical properties; Al_2O_3–YAG

1. Introduction

In recent years, considerable efforts have been made to develop high performance structural materials which can be used at high temperature with superior mechanical properties [1]. For several decades non-oxide ceramics such as SiC and Si_3N_4 have been developed as promising competitors to replace Ni-based superalloy. The room temperature brittleness, the high temperature instability and especially the serious oxidation above 1500 °C extremely restrict their application.

Oxide/oxide composites are being considered for long-term high temperature operations in an air environment. These composites require thermo-chemical compatibility with their application environment as well as thermo-mechanical compatibility with each other [2]. Creep behavior and mechanical properties of alumina ceramics can be improved by dispersing yttrium aluminum garnet (YAG) inclusion in the alumina matrix [3,4]. It was reported that the bending strength of YAG/Al_2O_3 composites at room temperature – around 400 MPa – can be maintained almost up to the melting point of 2093 °C when the displacement speed is high [5–9]. Accordingly, YAG/Al_2O_3 has received much attention in high temperature applications.

The synthesis process of YAG/Al_2O_3 composites has an obvious impact on the powder characteristics. In other words, powders synthesized by different methods have different sintering behavior. Some articles study YAG/Al_2O_3 composites prepared by the directional eutectic crystallization [9–12]. On the other hand, a great deal of research has been made to synthesize ultra fine powders with particle size less than 100 nm. Nano-powders have significantly enhanced sintering rates and decreased sintering temperatures compared to micrometer–sized particles due to higher surface area [13–16].

Sol–gel technique is a promising method for the preparation of nano-sized inorganic powders with homogeneous mixture of several components at a molecular level [17,18]. It was used for the preparation of YAG/Al_2O_3 composite fibers [19]. Lach et al. [20] elaborated a new technique for Al_2O_3/YAG composites' preparation covering a broad range of YAG contents from 5 to 30 vol. %. The technique is based on precipitation of yttria

---

* Corresponding author. Tel.: +49 711 68568234; fax: +49 711 68568301.
E-mail address: frank.sommer@ifkb.uni-stuttgart.de (F. Sommer).

0272-8842/$36.00 © 2012 Elsevier Ltd and Techna Group S.r.l. All rights reserved.
doi:10.1016/j.ceramint.2012.02.070

precursor within alumina grain suspension. Microscopic observations reported by Lach et al. [20] revealed that YAG inclusion sizes were smaller than alumina grains. Hardness of these materials was higher than observed in case of pure alumina. The highest fracture toughness was observed in the composites of 10 and 20 vol. % YAG content sintered at 1500 °C and 1600 °C.

Authors have recently successfully developed Al_2O_3/YAG composites with low yttria dopant by hot-pressing and injection molding [21,22]. Studies in this material system show that only a small amount of the YAG phase of about 1 vol.% is enough to cover alumina grains and change the fracture behavior. Sommer showed that with careful heat treatment, both transgranular and intergranular fracture behavior can be observed resulting in Evans toughness of $3.5\,MPa\sqrt{m}$ and bending strength of 568 MPa [22]. Due to the low amount of YAG hardness still remains at a relatively high level of 1857 HV_{10}. With higher amount of YAG phase, composites are likely to benefit from microstructured refinement.

However, previous studies on forming methods for Al_2O_3/YAG composites used dry axial pressing [23] or isostatic pressing [24]. Only little work has been carried out on slip-casting of aqueous yttria and alumina mixtures [25,26]. Colloidal forming techniques such as slip-casting are promising processes for manufacturing of Al_2O_3/YAG ceramics. Defects such as aggregates and agglomerates can be managed by preparation and dispersion techniques [27,28]. Li and Li [25] and Appiagyei et al. [26], revealed in their studies that high density and homogeneous microstructure YAG ceramics can be prepared by using slip casting forming method and vacuum sintering technique. Li and Li [25] described the effect of the dispersant agent concentration and pH value on the stability of the YAG aqueous slurry. While Appiagyei et al. [26] correlated the optical characteristics of vacuum sintered YAG ceramics with the dispersion properties of alumina and yttria mixture.

In the present work, Al_2O_3/YAG composites with YAG contents of 5, 10, and 20 vol.% were prepared using two different routes of preparation. In the first one, nano-sized YAG was prepared by sol–gel technique and then mixed with alumina. The second method was performed by coating of alumina grains with yttria in the proper concentration to get the required Al_2O_3/YAG composites. Slip-casting technique was used to prepare the green bodies of Al_2O_3/YAG composites. Mechanical properties of the densified composites were correlated to the microscopic and physical investigations.

2. Experimental

In the 1st processing route previously produced YAG powder [29] was attrition milled with zirconia balls until the D_{50} particle size was reduced to 1 μm. The change of particle size distributions with increasing milling time was investigated by laser granulometry (Malvern Lasersizer). For the slip-casting process three different aqueous slurries were prepared, consisting of an α-alumina (Sasol, North America, $S_{BET} = 8\ m^2/g$, $d_{50} = 0.3\ \mu m$) and 5, 10 and 20 vol.% of the milled YAG powder. For homogenization the slurry was gentle milled with 5 mm zirconia balls on a roll mixer for 20 h.

In the 2nd processing route an adequate amount of Y_2O_3 (99.99%, Sigma Aldrich) was dissolved in HNO_3 (5 M) and blended with the above mentioned α-alumina in isopropanol for the formation of 5, 10 and 20 vol.% Al_2O_3–YAG composites. After 24 h gentle milling with 5 mm zirconia balls the slurry was dried, crushed and screened with a 100 μm sieve. Subsequent calcination at 1200 °C for 30 min in air was carried out. Before slip-casting the coated powder was attrition milled for 3 h with 5 mm zirconia balls in distilled water in order to destroy the agglomerates, which were formed during the calcining step. Laser granulometry of the composite powders were carried out before and after milling.

The stabilization of aqueous Al_2O_3–YAG and YAG slurries has already been reported in the literature [20,25]. According to the literature 0.5 wt.% of ammonium polyacrylate was added to the aqueous suspension, consisting of 60 wt.% solid loading each. Two wt.% of binder (Zschimmer & Schwarz Octapix AC95) and one wt.% of plasticizer (Zschimmer & Schwarz Zusoplast 126/3) guaranteed required green strength and non-cracked samples.

Before slip-casting of 45 mm × 35 mm × 6 mm samples all slurries were placed in a vacuum chamber on a magnetic stirrer and evacuated to ~100 mbar until no air bubbles were detectable so that non-porous samples could be casted. The samples were then dried in a drying chamber and debinded with a two-step debindering program. First with a slow heating rate of 10 K/h up to 400 °C in order to smoothly remove the additives, second a higher heating rate of 120 K/h up to 800 °C with 30 min dwell to pre-sinter the samples for save handling.

The porosity distribution of the 10 vol.% YAG–Al_2O_3 presintered green bodies were monitored by mercury intrusion porosimetry (Pascal 140/440, Porotec GmbH, Germany), the microstructure of fractured green bodies was investigated by SEM (Leo VP 438) in order to detect inhomogeneities in the microstructure. All samples were subsequently sintered in air (Thermconcept HTK 16/17, Dr. Fischer GmbH & Co. KG Bremen, Germany). Dwell times varied from 1 to 3 h at a sintering temperature of 1500 °C and a heating rate of 2 K/min. After sintering, the samples were fine ground with a 40 μm diamond disk before polishing with 15, 6, 3 and 1 μm diamond suspension.

The density of all specimens was determined by the Archimedes method. For 3-point bending tests five test bars each of the polished samples were cut and the edges of the samples were carefully bevelled. Bending tests were performed according to DIN EN 6872. Microhardness (HV0.1) was tested with a Fischerscope microindenter on a polished surface (Fischer, Sindelfingen, Germany). The indentation modulus was calculated from the indentation curve according to the universal hardness method. Hardness (HV_{10}) was measured with the Vickers indentation method whereupon fracture toughness was calculated with the formula of Anstis and Evans from the length of the cracks of the HV_{10} measurements. Microstructures of sintered samples were studied by SEM (Zeiss, DSM982 Gemini, Germany) at 10,000× magnification,

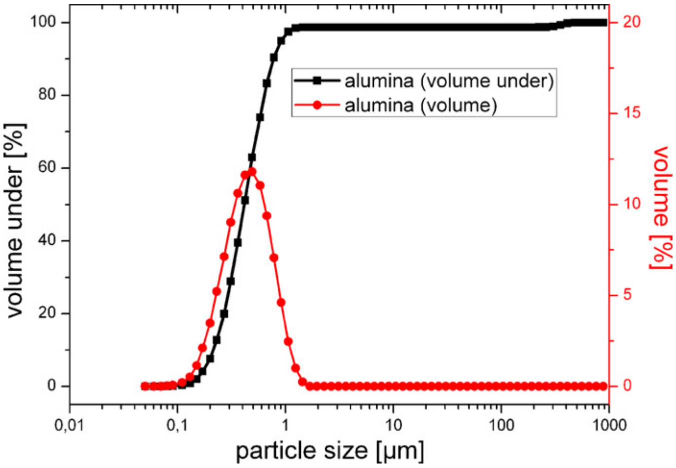

Fig. 1. Laser granulometry measurements of alumina starting powder.

YAG powders were studied by TEM (JEOL, JEM 1230, Japan) at 120 k× magnification.

3. Results and discussion

Laser granulometry measurements of the starting alumina powder showed a monomodal distribution with a D_{50} value of 0.41 µm (Fig. 1). Previous studies showed that this narrow size distribution cannot be shifted to finer particle sizes with further attrition milling without unfavorable debris of the milling media [21].

TEM pictures of the initial YAG powder were carried out. Fig. 2 illustrates primary particle sizes of ~20 nm of the initial YAG powder.

In comparison, laser granulometry measurements of the initial YAG powder showed a very broad particle size distribution including particles with large size, indicating that primary YAG particles in nanometer size are strongly agglomerated. Thus milling was carried out in order to break down agglomerates of the initial YAG powder. First the YAG powder was attrition milled for 2.5 h in isopropanol with 5 mm diameter ZrO_2 milling balls at 500 rpm. The amount of milling balls was selected equivalent to the volume of the YAG powder. While D_{10} kept approximately constant the D_{50} value was reduced from originally 12.06 µm to 5.27 µm, the D_{90} value was reduced from 93.21 µm to 15.98 µm, respectively. The accuracy of the measurement is ±2% according to the manufacturer's specification. Then further milling with 1 mm ZrO_2 balls was performed. Because the YAG powder was heavily agglomerated the powder was attrition milled up to 10 h at 500 rpm. Fig. 3 shows granulometry measurements after 2 h milling time each. Final D_{50} value was 0.67 µm with a quite monomodal particle distribution. In fact, the small peak in the 5 µm range should be attributed to soft agglomerates. These are probably found by reagglomeration during ultrasonic treatment prior to the measurement because the present shoulder strongly varies with ultrasonification time and no coarse YAG particles were detectable in the final microstructure.

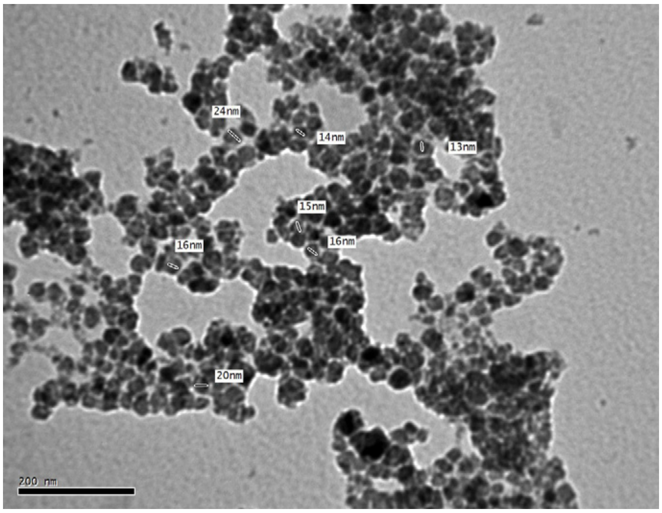

Fig. 2. TEM image of the initial YAG powder.

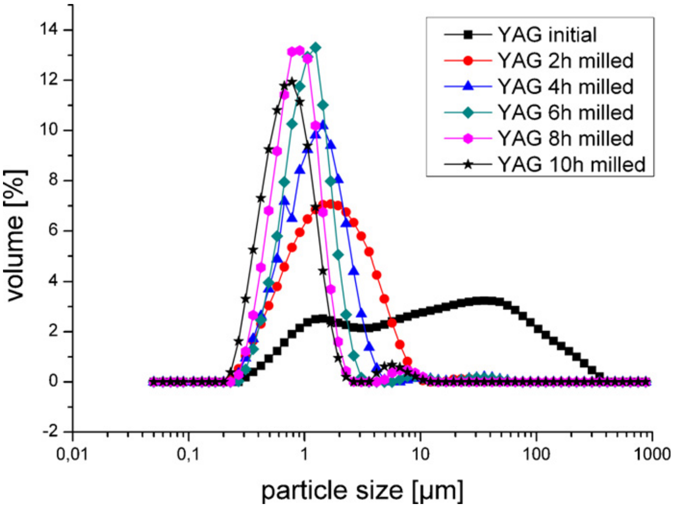

Fig. 3. Particle size distribution of YAG powder with increasing milling time.

For the second route of sample preparation granulometry measurements were carried out of the calcined 5, 10 and 20 vol.% YAG coated alumina before and after 3 h attrition milling with 5 mm diameter ZrO_2 milling balls at 500 rpm. Results show a D_{50} value of ~1 µm. Composite powders were not heavy agglomerated and showed quite monomodal particle distributions after the milling process (Fig. 4). A detectable shoulder at about 5–10 µm remains, indicating that a small content of coarse agglomerates still remains after the milling process. In comparison to the YAG powder, composite powder distributions were broader, which could be beneficial for green density.

Samples of both processing routes were casted, dried and subsequently debindered in air. First with heating rate of 10 K/h up to 400 °C, second with a rate of 120 K/h up to 800 °C with 30 min dwell to pre-sinter the samples for save handling.

The porosity distribution of the pre-sintered green bodies of 10 vol. % YAG–Al_2O_3 (coated and mixed) (Pascal 140/440, Porotec GmbH, Germany) showed that pore radii of the samples were between 0.023 and 0.076 µm (Figs. 5 and 6). Theoretically a homogenous monomodal packing of 0.3 µm

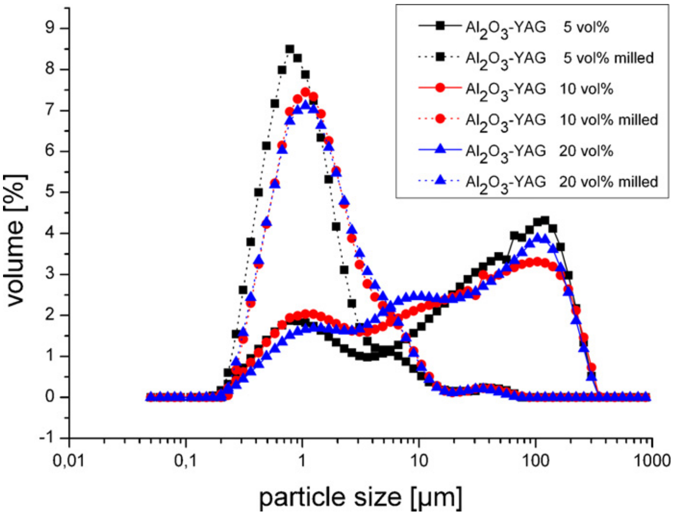

Fig. 4. Particle size distribution of alumina–YAG 5–20 vol.% powder before and after 3 h milling.

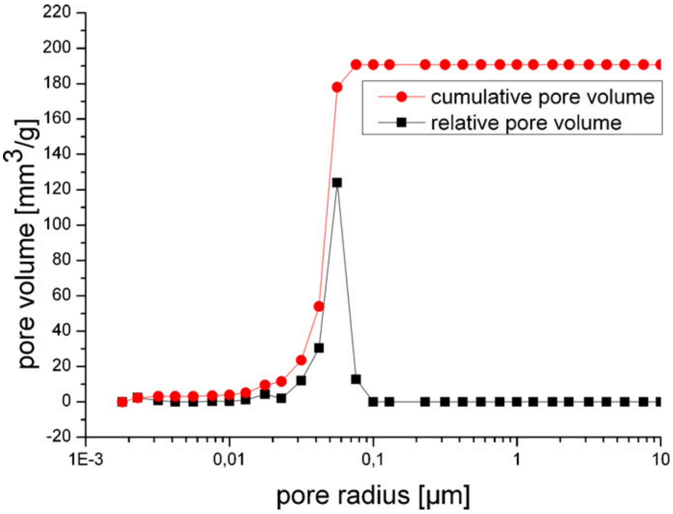

Fig. 6. Pore size distribution of coated alumina–YAG composite (route 2).

nonagglomerated spheres would result in a 0.07–0.12 µm spacing, respectively. The very fine part below 0.3 µm, which was noticeable in the particle size distribution should be responsible for even smaller pore radii measured than theoretical. The arrangement of a single narrow peak hints at a defect-free microstructure in both cases.

SEM (Leo VP 438) image (Fig. 7) of the presintered fracture face of the 1st processing route shows some pores, which has already been detected by mercury intrusion. Presintered image of the 2nd processing route shows similar fracture face. Large agglomerates were neither identified in mixed nor in coated composites.

Palmero reported that the formation of YAG from yttria coated alumina during calcining is very sensitive to the heat treatment [30]. Depending on the heat treatment intermediate phases like YAP ($YAlO_3$) and YAM (Y_4Al2O_9) can be formed, which are stable phases of the alumina–yttria phase system. Fig. 8 shows characteristic XRD patterns of 5–20 vol.% YAG coated alumina after calcining at 1200 °C at 30 min dwell in air. Peaks indicate the α-alumina phase (JCPDS 46-1212) as well as intermediate phases. Yttria phase was not found in any composition. The formation of the YAG phase during the calcination step varies with the amount of yttria. In the composition with lowest dopant content, only YAP and YAG were detected. However, one should keep in mind that reflexes are small due to the low dopant content. In 10 and 20 vol.% YAG coated alumina still differences are noticeable. While mainly intermediate YAP (JCPDS 33-0041) and YAM (34-0368) phases were detected in the 10 vol.% YAG composition most part of the composite already formed into the YAG (JCPDS 33-0040) structure in the 20 vol.% YAG composition.

For both processing routes small traces of the intermediate phases were found after sintering at 1500 °C with 2 K/min heating rate and 2 h soaking time. In coated composites parts of YAM and YAP phases remain. The existing content of intermediate phases of the calcined powders seems too high for final YAG transformation during sintering. Longer calcination times can be beneficial for complete YAG formation in the final composite. Mixed composites only reveal little YAP

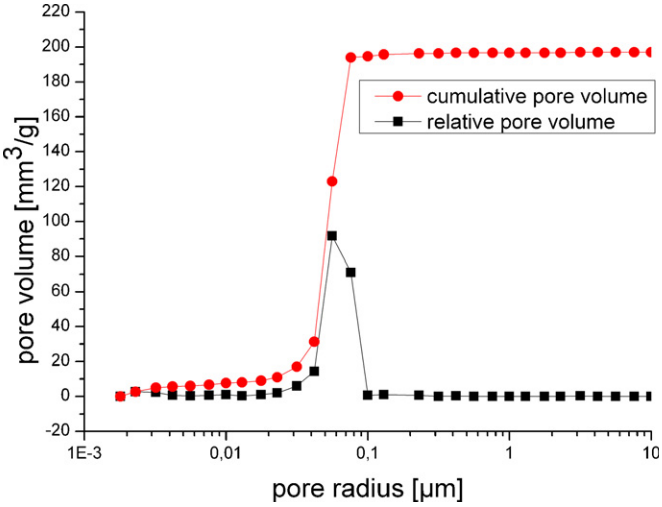

Fig. 5. Pore size distribution of mixed alumina–YAG composite (route 1).

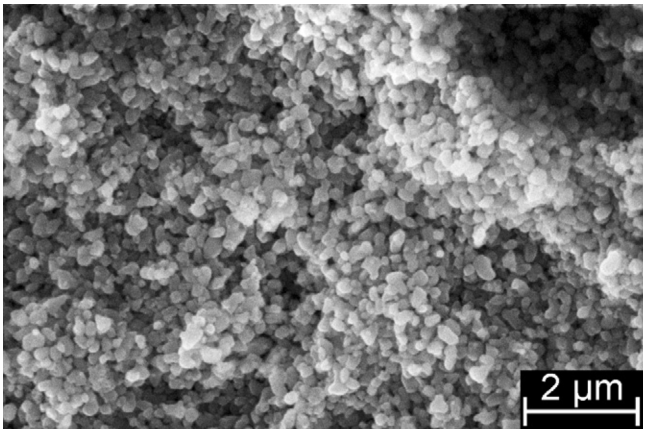

Fig. 7. SEM image of presintered fracture face of alumina 10 vol.% mixed YAG composite (route 1).

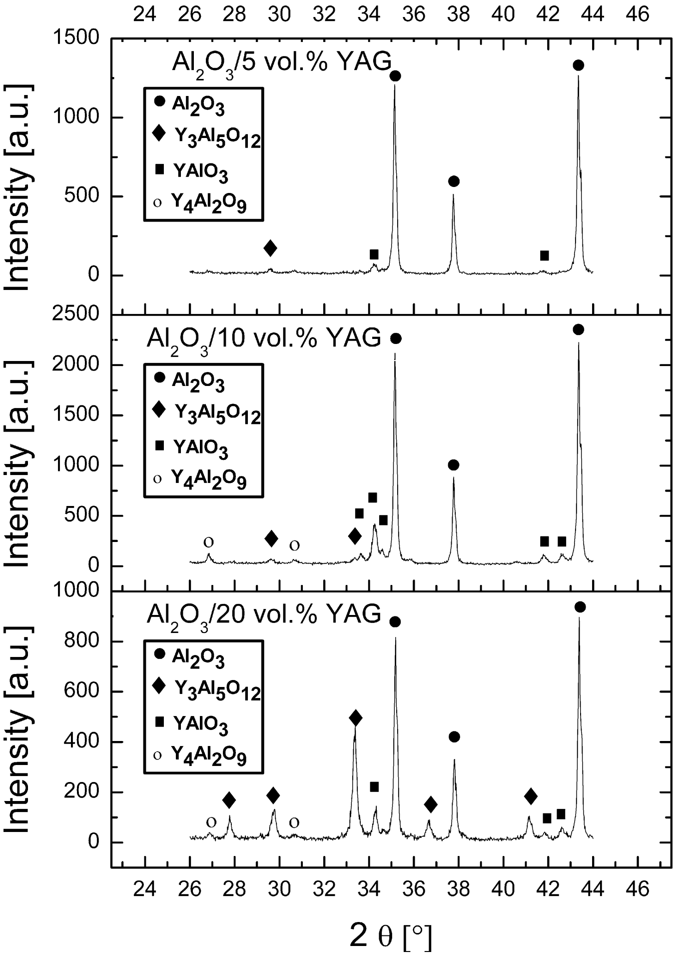

Fig. 8. XRD analysis of 5–20 vol.% YAG coated alumina after calcining.

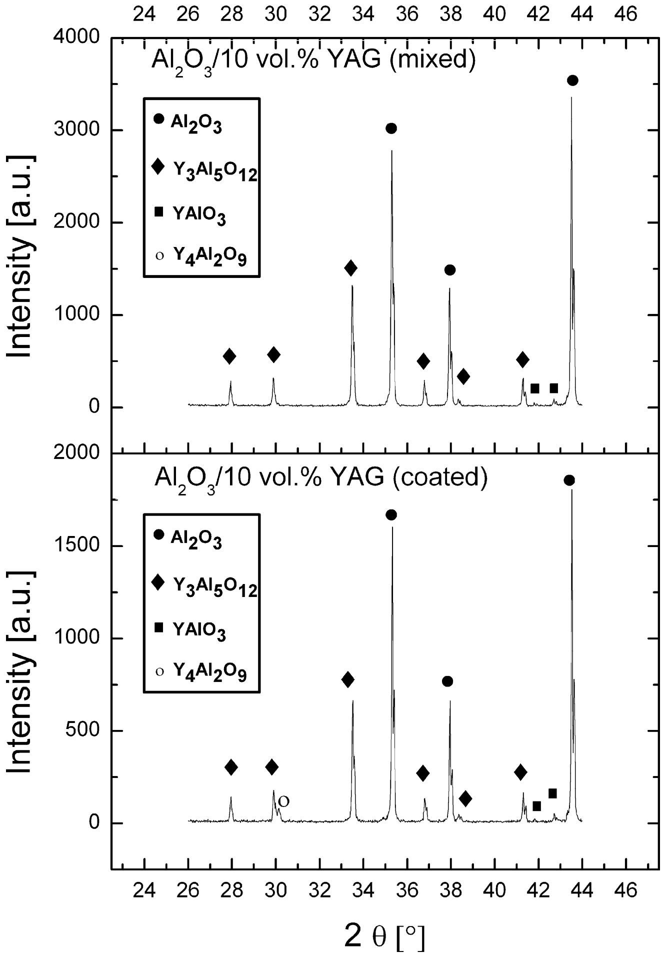

Fig. 9. XRD analysis of alumina/10 vol.% YAG composites after sintering at 1500 °C, 2 K/min, 2 h dwell (mixed and coated route).

phase presumably due to the beneficial heat treatment of the initial YAG powder. Fig. 9 illustrates characteristic XRD patterns of 10 vol.% alumina–YAG composites. Main peaks indicate the α-alumina and YAG phase.

Microstructures of thermally etched polished faces and fracture faces are demonstrated in Fig. 10. It shows Al_2O_3/10 vol.% YAG composites sintered in air at 1500 °C for 2 h dwell and 2 K/min heating rate, prepared either by the mixing (Fig. 10a and b) or coating route (Fig. 10c and d). Images of polished surfaces show a quite homogenous intergranular YAG distribution within the alumina matrix for coated composites. YAG distribution in mixed composites is inferior. Because YAG grains are not homogenously settled along grain boundaries, grain growth inhibition is limited. Alumina grains grow around YAG grains resulting in inter- but also intragranular fraction of YAG grains in mixed composites. YAG precipitates in coated composites are more fine-grained compared to mixed composites, which can also the reason for a finer alumina matrix. Microstructures of fracture faces show mainly intergranular fracture mode. When alumina grains grow partly transgranular fracture is noticeable.

The sintering parameters were set to 1500 °C, a dwell time between 1 and 3 h and 2 K/min heating rate. Al_2O_3 5 vol.% YAG samples produced by the mixing route reveal relative densities above 96%, independent on sintering time (Fig. 11). Highest micro- and macrohardness were measured for 1 and 2 h sintered samples, which correlates to the highest density (Fig. 12). Both, K_{1c} (Evans) and bending strength did not change significantly with different dwell times. Al_2O_3 10 vol.% YAG composites generally reveal higher densities, which results in higher macrohardness of 1785 HV10 for 1 h dwell. At longer dwell micro- and macrohardness decreases while bending strength reaches the highest value of 455 MPa at 3 h dwell (Fig. 13). The refinement in microstructure due to the higher amount of YAG seems to be the reason for higher bending strength. Increasing the YAG content from 10 vol.% to 20 vol.% did not further enhance the mechanical properties. All measured mechanical properties like bending strength, fracture toughness or hardness did not accomplish values of 10 vol.% YAG composites. Two reasons should be taken into consideration. One is the difficulty to homogeneously distribute the YAG phase within the alumina. A YAG content of 20 vol.% is above the percolation threshold of ~16 vol.%. When agglomerates are formed during shaping process the principle of microstructure refinement is limited. Second one should consider the high creep resistance of the YAG phase, which also hinders

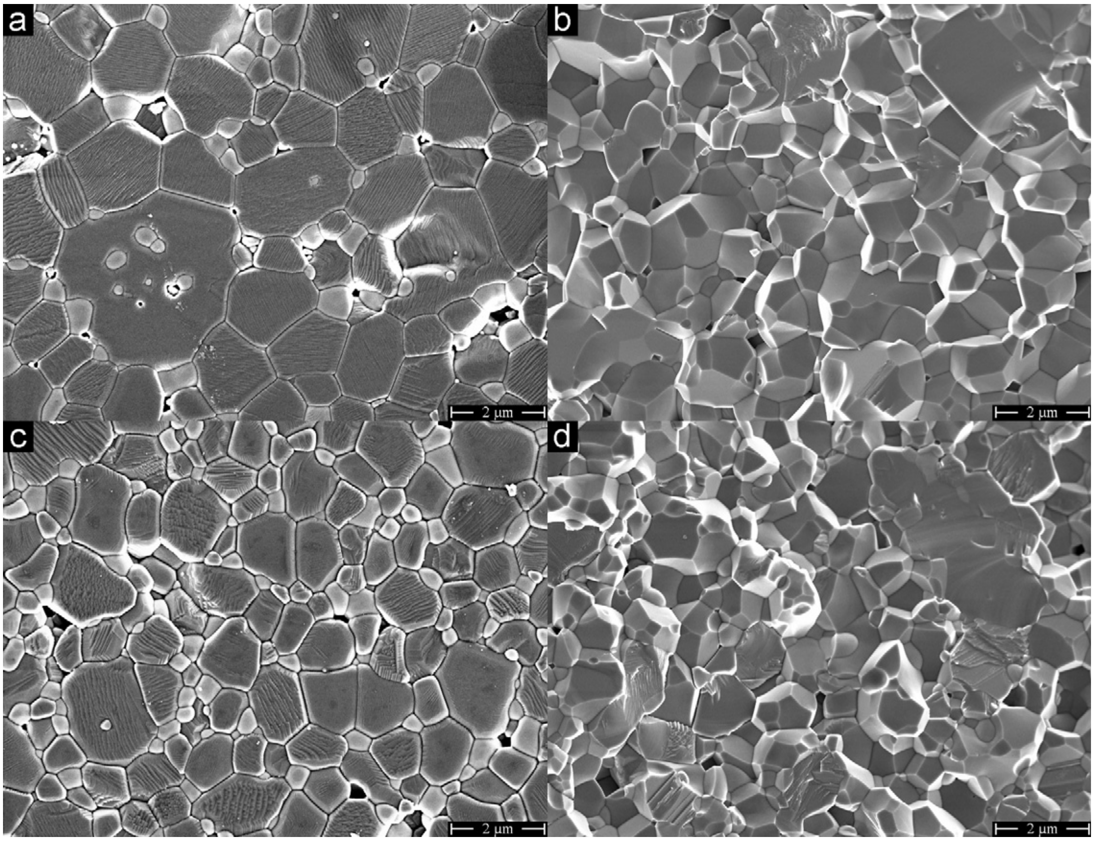

Fig. 10. Microstructure of Al_2O_3/10 vol.% YAG composites sintered at 1500 °C for 2 h dwell and 2 K/min heating rate in air: (a, b) prepared by mixing route; (c, d) prepared by coating route.

densification of the samples at the chosen sintering temperature.

Samples produced by the coating processing route reveal a different sintering behavior. Coated composites generally need longer dwell times to achieve comparable densities (Fig. 14). This should be attributed to the homogenous YAG layer on alumina particles which is formed during calcination and hinders the diffusion, hence densification. Such phenomenon has been studied and published by MacLaren, et al. [31]. They reported that the incorporation of Si and Y into grain boundaries cause the formation of very thin disordered regions. These disordered regions increase the mobility of the boundaries, yielding fast growth rates for some grains and abnormal grain size distribution. Remaining excess of yttria of also forms YAG

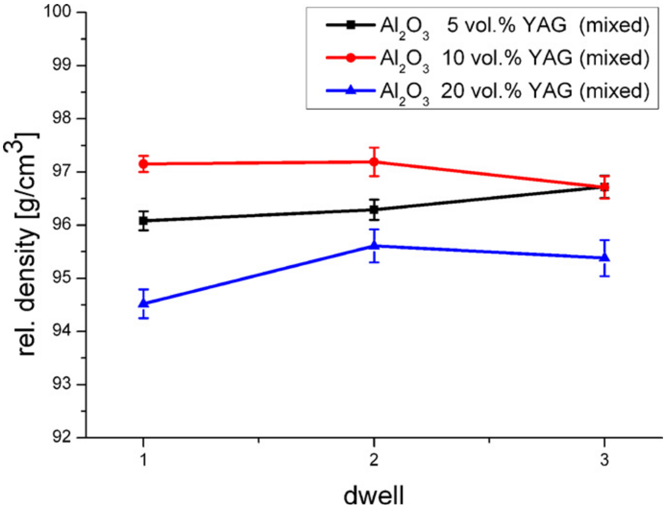

Fig. 11. Relative densities of Al_2O_3 5–20 vol.% YAG composites prepared by mixing route.

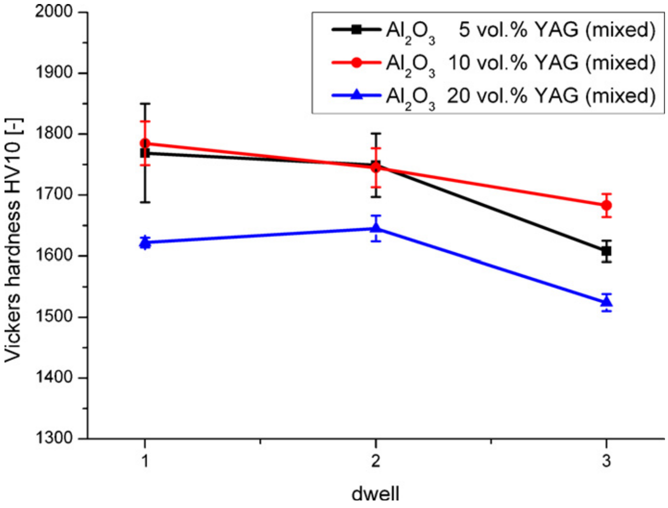

Fig. 12. Hardness HV10 of Al_2O_3 5–20 vol.% YAG composites prepared by mixing route. gr12.

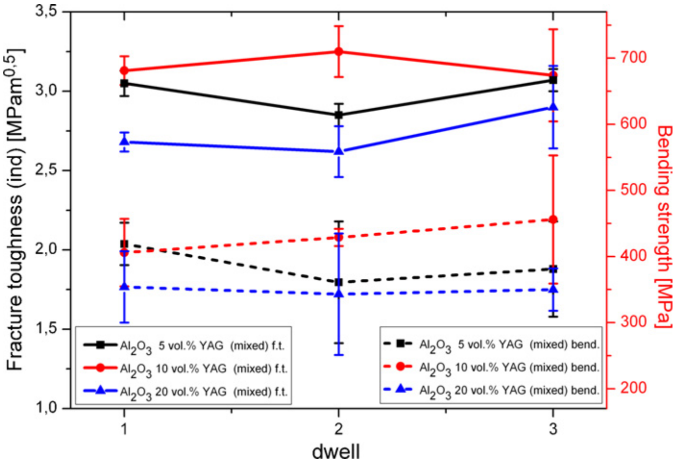

Fig. 13. Fracture toughness and bending strength of Al_2O_3 5–20 vol.% YAG composites prepared by mixing route.

grains, which settle along grain boundaries or triple points. The low hardness of 10 vol.% YAG composites can be attributed to the low relative density achieved. When densities of coated composites are on the same level to mixed composites, hardness level of both composites are comparable (Fig. 15). The ISB or SEVNB fracture toughness method are, in comparison to the fracture toughness measurements by indentation, well accepted in the literature. When material system and fracture behavior do not change in a study, fracture toughness values by indentation method still provide useful trends for comparison. However fracture toughness results of this study should only be compared to the same fracture toughness principle, model and material system of other studies.

Toughness values of coated composites (Fig. 16) are similar to toughness values of mixed composites. No explicit difference is noticed. Highest toughness values were measured for alumina 10 vol.% YAG composites with a Evans toughness of 3.25 MPa$\sqrt{}$m for the mixed composite sintered for 2 h dwell. Increasing the volume percentage of the YAG phase did neither improve strength nor toughness but causes significant decrease in macrohardness of composites because of the lower hardness of polycrystal YAG.

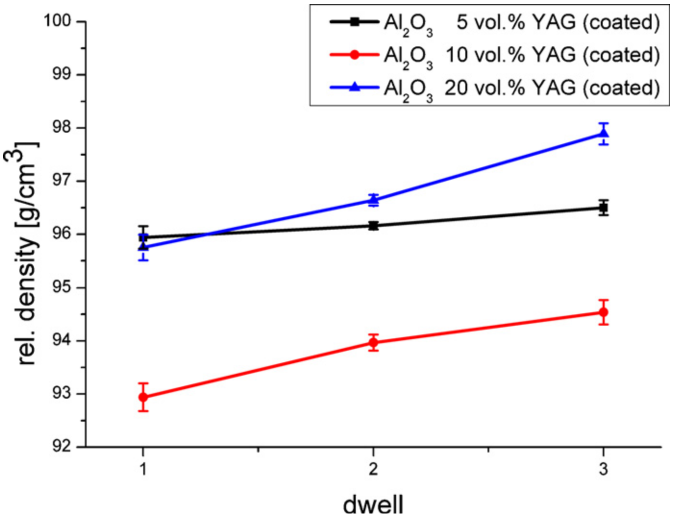

Fig. 14. Relative densities of Al_2O_3 5–20 vol.% YAG composites prepared by coating route.

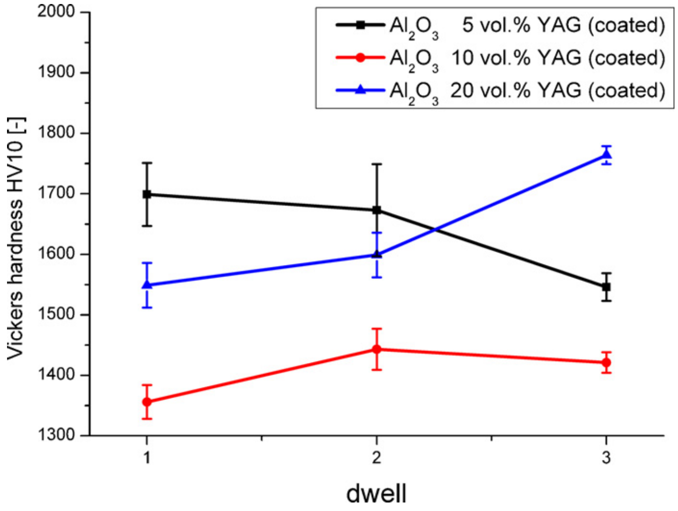

Fig. 15. Hardness HV10 of Al_2O_3 5–20 vol.% YAG composites prepared by coating route. gr15.

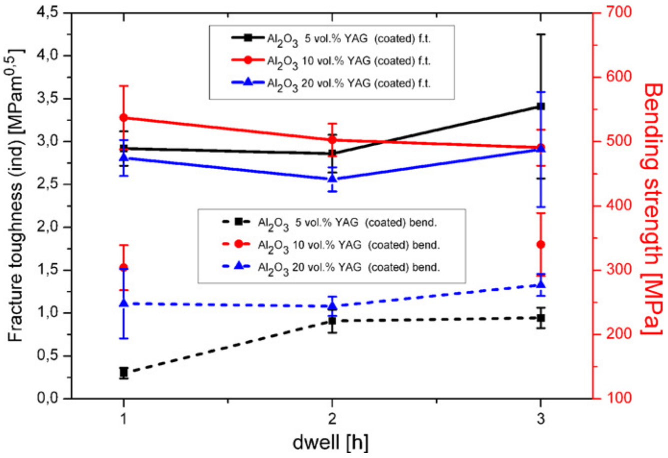

Fig. 16. Fracture toughness and bending strength of Al_2O_3 5–20 vol.% YAG composites prepared by coating route.

4. Conclusions

Alumina composites containing 5, 10 and 20 vol.% YAG were produced by a slip-casting process. Two different routes for the introduction of the YAG phase were chosen. Either by mixing previously produced YAG powder with Al_2O_3 or by coating alumina powders with yttria and subsequent calcination in order to generate YAG precipitates. Independent from the route of YAG introduction Al_2O_3/10 vol.% YAG composites show best mechanical properties. Mixed composites sintered at 1500 °C for 2 and 3 h dwell exhibit a bending strength of 428 MPa and 455 MPa and an Evans indentation toughness of 3.3 MPa$\sqrt{}$m and 3.1 MPa$\sqrt{}$m, respectively. Further addition of YAG did not increase mechanical properties, mainly because diffusion is hindered by YAG particles and thus samples exhibit lower densities at the chosen sintering parameters. This is also why coated composites reveal a different sintering behavior. The YAG layer on alumina particles results in slower densification rates and lower mechanical properties.

Composite composition of Al_2O_3–YAG ceramics have to be correctly adjusted depending on the purposes needed. If high strength and toughness are required, it is questionable to add more than 10 vol.% of the YAG phase. More than 10 vol.% of YAG phase did not improve properties in this study. This result is in accordance with the results published by Lach et al. [20]. No change in microstructure can be observed but densification becomes more difficult resulting in lower densities and hardness. Therefore higher amounts of YAG phase will mainly improve creep stability. Especially coated Al_2O_3–YAG composites should be advantageous to mixed composites if creep resistance is decisive. However, the processing of such coated alumina/YAG composites is considerably more complex regarding the casting and sintering behavior. If the processing can be optimized, the coating route has high potential as one can assume higher mechanical properties compared to the mixing route.

Acknowledgment

This work was supported by German-Egyptian Scientific Projects (GESP) fund (Grant ID: 1388).

References

[1] K. Hirano, Application of eutectic composites to gas turbine system and fundamental fracture properties up to 1700 °C, J. Eur. Ceram. Soc. 25 (2005) 1191.

[2] E.L. Courtright, Engineering property limitations of structural ceramic composites above 1600 °C, Ceram. Eng. Sci. Proc. 12 (1993) 1725–1744.

[3] R. Torrecillas, M. Schehl, L.A. Diaz, J.L. Menendes, J.S. Moya, Creep behaviour of alumina/YAG nanocomposites obtained by colloidal processing route, J. Eur. Ceram. Soc. 27 (2007) 143–150.

[4] W.Q. Li, L. Gao, Processing microstructure mechanical properties of 25 vol.% YAG–Al_2O_3 nanocomposites, Nanostruct. Mater. 11 (1999) 1073–1080.

[5] Y. Waku, N. Nakagawa, H. Otsubo, Y. Ohsora, Y. Kohtoku, High temperature properties of unidirectionally solidified Al_2O_3/YAG composites, J. Jpn. Inst. Met. 59 (1995) 71–78.

[6] Y. Waku, N. Nakagawa, T. Wakamoto, H. Otsubo, K. Shimizu, Y. Kohtoku, Excellent high-temperature properties of YAG Matrix composites reinforced with sapphire phases, in: T.S. Srivatsan, J.J. Moore (Eds.), Processing and Fabrication of Advanced Materials IV,, The Minerals, Metals and Materials Society, Warrendale, PA, 1996 , pp. pp323–pp339.

[7] Y. Waku, H. Otsubo, N. Nakagawa, Y. Kohtoku, Sapphire matrix composites reinforced with single crystal YAG phases, J. Mater. Sci. 31 (1996) 4663–4670.

[8] H. Yoshida, K. Shimura, S. Suginohara, Y. Ikuhara, T. Sakuma, N. Nakagawa, et al., High-temperature deformation in unidirectionally solidified eutectic Al_2O_3–YAG single crystal, Key Eng. Mater. 171-174 (2000) 855–862.

[9] S. Ochiai, T. Ueda, K. Sato, M. Hojo, Y. Waku, N. Nakagawa, et al., Deformation and fracture behavior of Al_2O_3/YAG composite from room temperature to 2023 K, Compos. Sci. Technol. 61 (2001) 2117–2128.

[10] T. Mah, T.A. Parthasarathy, L.E. Matson, Processing mechanical properties of $Al_2O_3/Y_3Al_5O_{12}$ (YAG) eutectic composites, Ceram Eng Sci. Proc. 11 (1990) 1617.

[11] Y. Harada, T. Suzuki, K. Hirano, Y. Waku, Ultra-high temperature compressive creep behavior of an in-situ Al_2O_3 single crystal/YAG eutectic composite, J. Eur. Ceram. Soc. 24 (2004) 2215–2222.

[12] J. Ramirez-Rico, A.R. Pinto-Gómez, J. Martinez-Fernandez, A.R. De Arellano-López, P.B. Oliete, J.I. Pena, et al., High temperature plastic behavior of Al_2O_3–$Y_3Al_5O_{12}$ directionally solidified eutictics, Acta Mater. 54 (2006) 3107–3116.

[13] S.C. Tjong, H. Chen, Nanocrystalline Materials, Coatings, Mater. Sci. Eng. Rep. 45 (2004) 1–88.

[14] M.J. Iqbal, M.N. Ashiq, Comparative studies of $SrZr_XMn_XFe_{12-2X}O_{12}$ nanocomposites synthesis by co-precipitation and sol–gel combustion methods, Scr. Mater. 56 (2007) 145–148.

[15] J. Markmann, A. Tschope, R. Birringer, Low temperature processing of dense nanocrystalline yttrium-doped cerium oxide ceramics, Acta Mater. 50 (2002) 1433–1440.

[16] P. Palmero, A. Simone, C. Esnout, G. Fantozzi, L. Montanaro, Comparison among different sintering routes for preparing alumina–YAG nanocomposites, J. Eur. Ceram. Soc. 26 (2006) 941–947.

[17] S.A. Hassanzadeh-Tabrizi, E. Taheri-Nassaj, H. Sarpoolaky, Synthesis of an alumina–YAG nanopowder via sol–gel method, J. Alloys Compd. 456 (2008) 282–285.

[18] S.A. Hassanzadeh-Tabrizi, E. Taheri-Nassaj, Effect of milling and calcination temperature of the compressibility and sinterability of nanocrystalline Al_2O_3–$Y_3Al_5O_{12}$ composite powder, J. Am. Ceram. Soc. 91 (11) (2008) 3546–3551.

[19] K. Okada, T. Motohashi, Y. Kameshima, A. Yasumori, Sol–gel synthesis of YAG/Al_2O_3 long fibres from water solvent systems, J. Eur. Ceram. Soc. 20 (2000) 561–567.

[20] R. Lach, K. Haberko, M.M. Bućko, M. Szumera, G. Grabowski, Ceramic matrix composites in the alumina/5–30 vol.% YAG system, J. Eur. Ceram. Soc. 31 (2011) 1889–1895.

[21] F. Sommer, F. Kern, R. Gadow, Hot-pressing of yttria–chromia alumina composites, Proc. CIEC, 12, Mons Belgium, S2 (2010).

[22] F. Sommer, F. Kern, R. Gadow, Injection molding of alumina–chromia–yttria composites, J. Ceram. Sci. Tech. 2 (2011) 211–216.

[23] G.S. Corman, High-temperature creep of some crystal oxides, Ceram. Eng. Sci. Proc. 12 (9,10) (1991) 1745–1766.

[24] A. Ikesue, T. Kinooshita, K. Kamata, Fabrication, Optical properties of high-performance polycrystalline Nd:YAG ceramics for solid-state lasers, J. Am. Ceram. Soc. 78 (1995) 1033–1040.

[25] X. Li, Q. Li, YAG ceramic processed by slip casting via aqueous slurries, Ceram. Int. 34 (2008) 397–401.

[26] K.A. Appiagyei, G.L. Messing, J.Q. Dumm, Aqueous slip casting of transparent yttrium aluminum garnet (YAG) ceramics, Ceram. Int. 34 (2008) 1309–1313.

[27] K. Chou, L. Lee, Effect of dispersant on the rheological properties and slip casting of concentrated alumina slurry, J. Am. Ceram. Soc. 72 (9) (1989) 1622–1627.

[28] J.A. Leurs, Colloidal processing of ceramics, J. Am. Ceram. Soc. 83 (10) (2000) 2341–2359.

[29] A. Katelnikovas, J. Barkauskas, F. Ivanauskas, A. Beganskiene, A. Kareiva, Aqueous sol–gel synthesis route for the preparation of YAG: evaluation of sol–gel process by mathematical regression model, J. Sol–Gel Sci. Technol. 41 (2007) 193–201.

[30] P. Palmero, V. Naglieri, J. Chevalier, G. Fantozzi, L. Montanaro, Alumina-based nanocomposites obtained by doping with inorganic salt solutions: application to immiscible and reactive systems, J. Eur. Ceram. Soc. 29 (2009) 59–66.

[31] I. MacLaren, R.M. Cannon, M.A. Gülgün, R. Voytovytch, N. Popescu-Pogrion, C. Scheu, U. Täffner, M. Rühle, Abnormal grain growth in alumina: synergistic effects of yttria and silica, J. Am. Ceram. Soc. 86 (2003) 650–659.